DOI: 10.1002/ange.201209991

Oral Delivery of siRNA

Supramolecular Self-Assembled Nanoparticles Mediate Oral Delivery of Therapeutic TNF-α siRNA against Systemic Inflammation**

*Lichen Yin, Ziyuan Song, Qiuhao Qu, Kyung Hoon Kim, Nan Zheng, Catherine Yao, Isthier Chaudhury, Haoyu Tang, Nathan P. Gabrielson, Fatih M. Uckun, and Jianjun Cheng**

Intervention of the inflammation cascade with tumor necrosis factor-α (TNF-α) monoclonal antibodies or receptors represents a major approach in clinical immunotherapy against inflammatory diseases, which however, often suffers from high cost, autoimmunity to antibodies, and various side effects.[1] siRNA-mediated RNA interference (RNAi) has recently emerged as a potent modality in regulating gene expression by suppressing mRNA translation;[2–13] its high efficiency and specificity has made it a promising treatment paradigm for TNF-α-mediated inflammatory disorders.[14–18] The therapeutic potential of siRNA was recently exemplified by a report of attenuating systemic inflammation by targeting orally delivered Map4k4 siRNA to gut-associated macrophages (GAMs).[19] Owing to the infiltration of GAMs to systemic reticuloendothelial tissues, Map4k4 siRNA-mediated TNF-α knockdown in GAMs extended to other tissues and thus induced systemic anti-inflammatory effects.[19]

Despite its biological potency, the clinical potential of orally delivered siRNA has been hampered by the lack of efficient delivery technologies. siRNA is anionic, hydrophilic, and easily degraded by nucleases in the body. As such, it cannot survive the harsh conditions of the gastrointestinal (GI) tract or effectively penetrate the intestinal epithelia or membranes of target cells.[20,21] Hence, an effective carrier is needed not only to protect siRNA from degradation in the GI tract but also to improve the intestinal absorption as well as transfection in macrophages,[22] thereby maximizing the in vivo RNAi efficiency and anti-inflammatory effect of orally delivered siRNA.

To address the dearth of techniques for oral siRNA delivery, here we report the design of supramolecular self-assembled nanoparticles (SSNPs) that are able to overcome the absorption and transfection barriers posed by intestinal macrophages and exhibit remarkable in vivo oral RNAi efficiency. SSNPs were constructed through the electrostatic and hydrophobic self-assembly of several rationally designed or selected building blocks,[23] including oleyl trimethyl chitosan (OTMC), poly(γ-(4-(((2-(piperidin-1-yl)ethyl)-amino)methyl)benzyl-L-glutamate) (PVBLG-8), oleyl-PEG-mannose (OPM), oleyl-PEG-cysteamine (OPC), sodium tripolyphosphate (TPP), and TNF-α siRNA (Figure 1 A).

Trimethyl chitosan (TMC) is an effective intestinal absorption enhancer as well as transfection reagent.[24] As a more hydrophobic derivative of TMC, OTMC with the oleyl conjugation ratio of 20.3 % was synthesized and expected to display further enhanced permeation-enhancing and gene transfection capabilities.[25] PVBLG-8 is a cationic α-helical polypeptide we recently developed[26,27] which exhibits potent membrane activities and gene delivery efficiencies. We incorporated PVBLG-8 (degree of polymerization (DP) = 195) into the SSNPs in attempt to promote the cellular internalization and endosomal escape. PVBLG-8 adopts a superstable α-helical structure between pH 2 and 9 (Figure S2 in the Supporting Information), making it an ideal material for oral delivery applications as it is able to maintain helical secondary structure after passing through both stomach (acidic) and intestinal (weakly basic) environments. Incorporating OPM is expected to target SSNPs to enterocytes and macrophages that express mannose receptors,[28] thus improving the intestinal absorption and macrophage uptake. OPC will improve the mucoadhesion of SSNPs by forming disulfide bonds with mucin glycoproteins enriched in the intestinal mucosa and on cell surfaces.[29] OPM and OPC were synthesized by conjugation methods and their structures were confirmed by MALDI-TOF mass spectrometry (Figures S3 and S4 in the Supporting Information). The 2′-*O*-methyl-modified siRNA duplex against TNF-α was reported previously,[14,30] wherein the 2′-*O*-methyl modification on the antisense strand eliminates off-target effects, minimizes non-specific immune responses, and improves siRNA stability. With these building blocks, SSNPs are expected to promote the intestinal absorption of TNF-α siRNA, facilitate RNAi in macrophages, and thus mediate systemic TNF-α knockdown against lipopolysaccharide (LPS)-induced hepatic injury.

For the construction of SSNPs, TNF-α siRNA was condensed with cationic OTMC and PVBLG-8 through

[*] Dr. L. Yin, Z. Song, K. H. Kim, N. Zheng, C. Yao, I. Chaudhury, Dr. H. Tang, Prof. Dr. J. Cheng
Department of Materials Science and Engineering
University of Illinois, Urbana-Champaign
1304 West Green Street, Urbana, IL 61801 (USA)
E-mail: jianjunc@illinois.edu
Homepage: http://cheng.matse.illinois.edu/
Dr. Q. Qu, Dr. N. P. Gabrielson
Institute of Genomic Biology
University of Illinois, Urbana-Champaign
1206 West Gregory Drive, Urbana, IL 61801 (USA)
Prof. Dr. F. M. Uckun
Division of Hematology-Oncology
Systems Immunobiology Laboratory
Children's Center for Cancer and Blood Diseases
Children's Hospital Los Angeles, Los Angeles, CA 90027 (USA)

[**] J.C. acknowledges support from the NSF (CHE-1153122) and the NIH (NIH Director's New Innovator Award 1DP2OD007246 and 1R21EB013379). TNF-α siRNA = tumor necrosis factor-α small interfering RNA.

Supporting information for this article is available on the WWW under http://dx.doi.org/10.1002/anie.201209991.

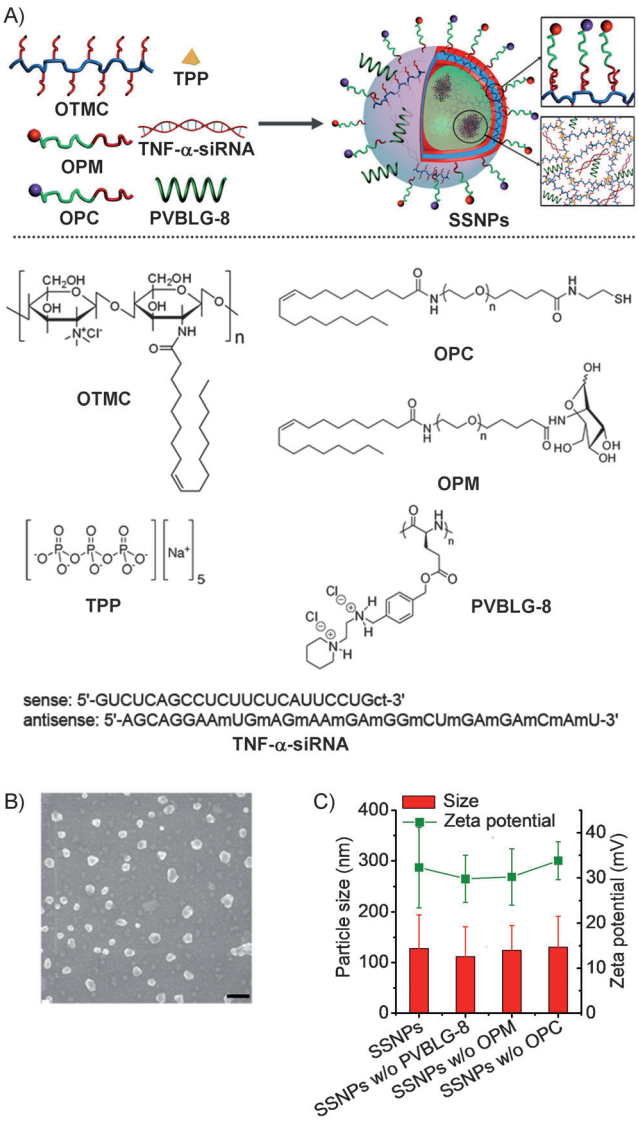

Figure 1. (A) Schematic illustration, (B) SEM image, and (C) particle size and zeta potential of SSNPs (bar = 200 nm in the SEM image).

electrostatic interactions at an OTMC/PVBLG-8/siRNA ratio of 100:20:1 (w/w). TPP, incorporated at an optimized TPP/OTMC ratio of 1:8 (w/w) (Figure S5 in the Supporting Information), served as an anionic cross-linker for OTMC to stabilize the complexes.[31] OPM and OPC were incorporated through intermolecular hydrophobic interactions with OTMC at a fixed ratio of 1:1:1 (w/w/w). The resulting SSNPs had a particle size of 128 nm, a zeta potential of 33 mV, and a spherical morphology (Figure 1 B, C). siRNA incorporation into the SSNPs was confirmed by a gel retardation assay, which revealed restricted migration of siRNA (Figure S6 in the Supporting Information). When PVBLG-8, OPM, or OPC was removed from SSNPs, the particle size and zeta potential remained unchanged (Figure 1 C), allowing comparison of the biological functions of SSNPs with their PVBLG-8-, OPM-, or OPC-depleted analogues.

The intestinal absorption of SSNPs and the associated mechanisms were examined in two in vitro models. The non-follicle-associated epithelia (non-FAE) model, obtained from monocultured Caco-2 cell monolayers, has been widely used as an in vitro intestinal epithelia model because the cultured Caco-2 cells differentiate into polarized, columnar cells and transporting epithelium with well-developed microvilli.[32] The FAE model, obtained from Caco-2 cell monolayers co-cultured with Raji B lymphocytes, additionally contains a distinctive M cell phenotype.[33] We monitored the apparent permeability coefficient (P_{app}) of Cy3-siRNA in these two models which represented the intestinal transport level. SSNPs enhanced siRNA transport in both models by 15–18-fold (Figure 2 A), which agreed well with their deeper penetration into the cell monolayers (Figure 2 B). Quantitative analysis of the images confirmed an increased depth of siRNA penetration from 3.2 μm (naked siRNA) to 33.8 μm (SSNPs) (Figure 2 C). We further noted a 2.9-fold improvement in siRNA transport in the FAE model compared to that in the non-FAE model for SSNPs (Figure 2 A), suggesting that a large proportion of the SSNPs were absorbed by transcellular uptake by M cells (pathway I, Figure 2 G), the most rapid and potent translocation pathway during intestinal absorption.

In addition to M cell uptake, we also evaluated the involvement of two other pathways, intracellular uptake by normal enterocytes (pathway II, Figure 2 G) and paracellular transport through tight junctions (TJs, pathway III, Figure 2 G). As shown in Figure 2 D and in Figure S7 in the Supporting Information, addition of the SSNPs at the apical side of the monolayers rapidly decreased the transepithelial electric resistance (TEER) values, suggesting that SSNPs opened the TJs to facilitate paracellular siRNA transport. The underlying mechanisms were explored by immunostaining the TJ-associated proteins (TJAPs), F-actin and ZO-1. Untreated cell monolayers showed uniformly distributed F-actin and continuous cell frame distribution of ZO-1 proteins (control, Figure 2 E; Figures S8 and S9 in the Supporting Information). Upon treatment of SSNPs, F-actin filaments were redistributed, shortened, and aggregated, and ZO-1 proteins appeared to be loosened and discontinuous (SSNPs), indicating that the SSNPs triggered the reconfiguration of TJAPs and opened the TJs.[34] After removal of SSNPs and further incubation for 24 h, the ZO-1 and F-actin patterns recovered to the untreated state (control), indicating reversible opening and restoration of epithelial TJs. In the non-FAE model containing only normal enterocytes, SSNPs markedly promoted the uptake of Cy3-siRNA (Figure 2 F), suggesting that SSNPs enhanced the transcellular uptake of siRNA by normal enterocytes. In these experiments, we noted significantly decreased siRNA transport and uptake in both models when PVBLG-8, OPM, or OPC were removed from the SSNPs (Figure 2 A, F). This observation validated our hypothesis that intestinal absorption of siRNA could be improved by OPM-mediated targeting of SSNPs to enterocytes and M cells, OPC-mediated intestinal mucoadhesion (Figure S10 in the Supporting Information), and PVBLG-8-mediated membrane permeation.

Since macrophages are the target cells for TNF-α siRNA-mediated gene silencing, we then explored the intracellular delivery and RNAi efficiency of SSNPs in RAW 264.7 cells. SSNPs markedly increased Cy3-siRNA uptake levels (Fig-

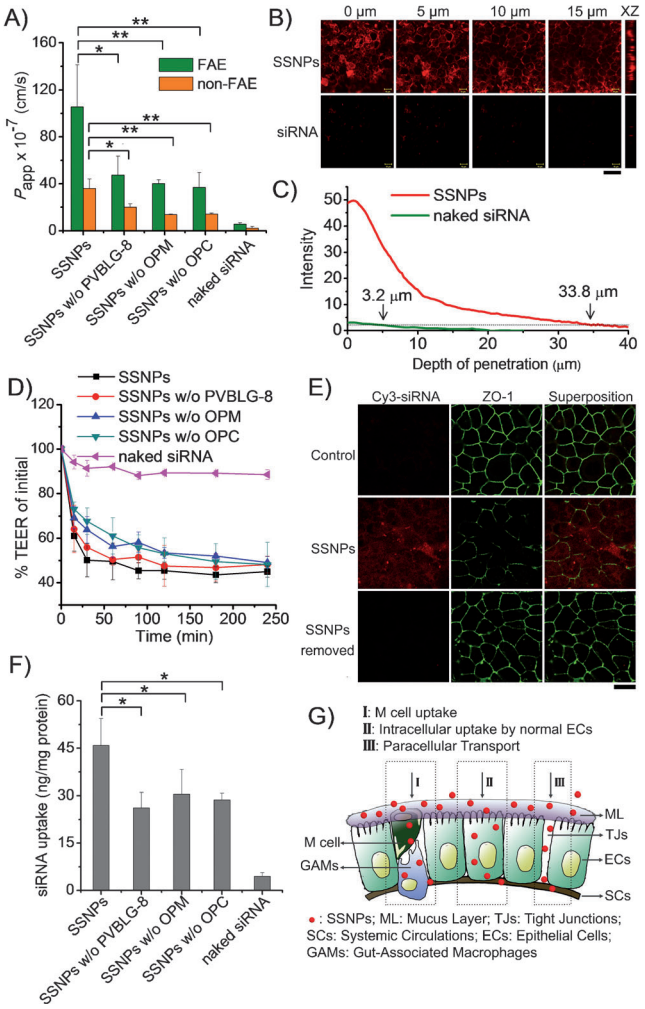

Figure 2. Intestinal absorption of Cy3-siRNA-containing SSNPs. A) P_{app} of Cy3-siRNA across human non-FAE and FAE models ($n=3$). B) Confocal laser scanning microscopy (CLSM) images showing cross-sections of the FAE model at 5 μm increments in the *z* direction following SSNP treatment for 4 h (bar = 20 μm). C) Penetration depth of Cy3-siRNA in the FAE model. D) TEER values of the FAE model following incubation with SSNPs ($n=3$). E) CLSM images of the FAE model stained for ZO-1 after treatment with SSNPs (bar = 20 μm). F) Uptake of SSNPs in the non-FAE model following 4 h incubation ($n=3$). () Intestinal absorption pathways of SSNPs, including transcellular transport by M cells (pathway I), uptake by normal enterocytes (pathway II), and paracellular transport through transiently opened tight junctions (pathway III). The absorbed SSNPs were transferred either to GAMs or to systemic circulation.

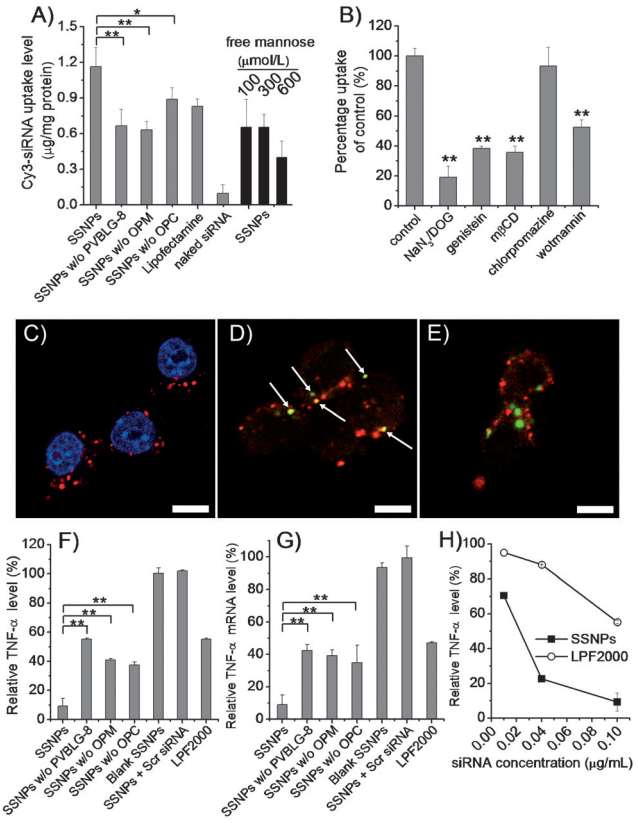

Figure 3. SSNPs deliver TNF-α siRNA to macrophages by means of mannose-receptor-mediated endocytosis and attenuate TNF-α production in vitro. A) Uptake of Cy3-siRNA-containing SSNPs in RAW 264.7 cells following incubation for 4 h ($n=3$). B) Uptake of SSNPs in RAW 264.7 cells in the presence of various endocytosis inhibitors ($n=3$). C) CLSM images showing internalization of Cy3-siRNA-containing SSNPs in RAW 264.7 cells. Cy3-siRNA-SSNPs co-localized with FITC-CTB (D, white arrows) rather than with transferrin–Alexa Fluor 635 (E; bar = 10 μm). Levels of TNF-α (F) and TNF-α mRNA (G) in RAW 264.7 cells following treatment with SSNPs at 0.1 μg siRNA mL^{-1}. H) Comparison on the TNF-α knockdown efficiencies of SSNPs and LPF2000/siRNA complexes at various siRNA doses ($n=3$).

ure 3A), and internalized Cy3-siRNA was observed in the cytoplasm (Figure 3C). When PVBLG-8, OPM, or OPC was removed from the SSNPs, the siRNA uptake level was significantly reduced, supporting our design strategy of enhancing macrophage uptake through PVBLG-8-mediated membrane penetration, OPM-mediated mannose-receptor recognition, and OPC-mediated cell binding. The mannose-receptor-mediated targeting effect was further verified by the reduced siRNA uptake level when free mannose was added to competitively occupy the mannose receptors (Figure 3A). Because RNAi efficiency is closely related to the intracellular kinetics, we also probed the internalization pathways of SSNPs using various endocytic inhibitors.[35] NaN_3/deoxyglucose (DOG) substantially reduced the uptake of SSNPs, suggesting that they were mainly internalized through energy-dependent endocytosis (Figure 3B). The caveolae inhibitors methyl-β-cyclodextrin (mβCD) and genistein and macropinocytosis inhibitor wortmannin[35] significantly suppressed SSNP uptake, indicating that both caveolae and macropinocytosis were involved in endocytosis. In contrast, chlorpromazine exerted an unappreciable inhibitory effect, suggesting irrelevance to clathrin-mediated endocytosis.[35] For further validation, we co-incubated Cy3-siRNA-containing SSNPs with transferrin–Alexa Fluor 635 or FITC–cholera toxin B (FITC-CTB) which are endocytosed by clathrin- and caveolae-mediated pathways, respectively.[35] Confocal laser scanning microscopy (CLSM) analysis showed that internalized SSNPs co-localized with CTB (Figure 3E) rather than with transferrin (Figure 3D), which confirmed the caveolae pathway for SSNP uptake. As a result of the efficient cellular uptake, SSNPs inhibited LPS-induced TNF-α production in RAW 264.7 cells by roughly 90% at a siRNA concentration of

0.1 μg mL^{-1} (Figure 3F,G). In agreement with the decreased uptake level, omission of PVBLG-8, OPM, or OPC from SSNPs resulted in a significant decrease in TNF-α knockdown efficiency. More noteworthy, SSNPs markedly outperformed Lipofectamine 2000 (LPF2000), exhibiting similar efficacy at an siRNA dose 10-fold less than that of LPF2000 (Figure 3H) and 20–100-fold less than that of other nonviral vectors reported.[15–17,36]

The ability of orally administered SSNPs to mediate systemic TNF-α knockdown and anti-inflammatory effect was evaluated in an LPS/D-GalN-induced murine hepatic injury model. The stability of SSNPs was first evaluated under simulated conditions. To mimic the pH change in the GI tract, the pH of the SSNPs suspension was adjusted from 6.8 (intestinal pH) to 1.2 (gastric pH) and then back to 6.8. The size and zeta potential of the SSNPs were unaffected by pH changes (Figure S14 in the Supporting Information), suggesting their stability during transit through the GI tract. Likewise, dilution of SSNPs with 0.15 M PBS (pH 6.8) up to 100-fold resulted in unappreciable change in their sizes and zeta potentials (Figure S15 in the Supporting Information), indicating that SSNPs can withstand the extensive dilution by physiological fluids. Following treatment with mouse serum or intestinal fluids, SSNPs effectively preserved the siRNA integrity (Figure S16 in the Supporting Information), substantiating their desired resistance against nuclease attack. The biodistribution profiles of orally delivered SSNPs were then evaluated by using DY800-siRNA. SSNP-treated mice experienced notably higher siRNA distribution levels in the liver, spleen, and lung than mice receiving naked siRNA (Figure 4A). Combined with the observation of a roughly 20-fold higher siRNA level in the small intestine, it was demonstrated that SSNPs promoted both intestinal absorption and systemic translocation of siRNA. Single gavage of SSNPs at a dose of 200 μg TNF-α siRNA kg^{-1} reduced mouse serum TNF-α levels by 80% (Figure 4B) and notably depleted TNF-α mRNA in macrophage-enriched organs (liver, spleen, and lung; Figure 4C), which suggested that the intestinally absorbed SSNPs had infiltrated and transfected macrophages in reticuloendothelial tissues to induce systemic TNF-α knockdown.[19] In accordance with the intestinal absorption levels and in vitro RNAi efficiencies, SSNPs without OPM, OPC, or PVBLG-8 showed significantly reduced in vivo silencing efficiency (Figure 4B,C), again substantiating the essential roles of individual components in mediating oral absorption and systemic gene knockdown. As a result of systemic TNF-α knockdown, orally delivered SSNPs displayed marked anti-inflammatory effects against LPS/D-GalN-induced acute hepatic injury. LPS/D-GalN challenge elevated serum levels of alanine transaminase (ALT) and aspartate aminotransferase (AST) (Figure 4D), and caused animal lethality within 12 h (Figure 4E). In comparison, SSNPs orally administered 24 h before LPS/D-GalN stimulation significantly inhibited the elevation in serum ALT/AST levels and improved the survival rate. During necropsy, we noticed that livers from control mice (only LPS/D-GalN treated) had turned yellow or black, indicating severe lipid accumulation, liver steatosis, and hemorrhage. While for SSNPs-treated mice, most of the

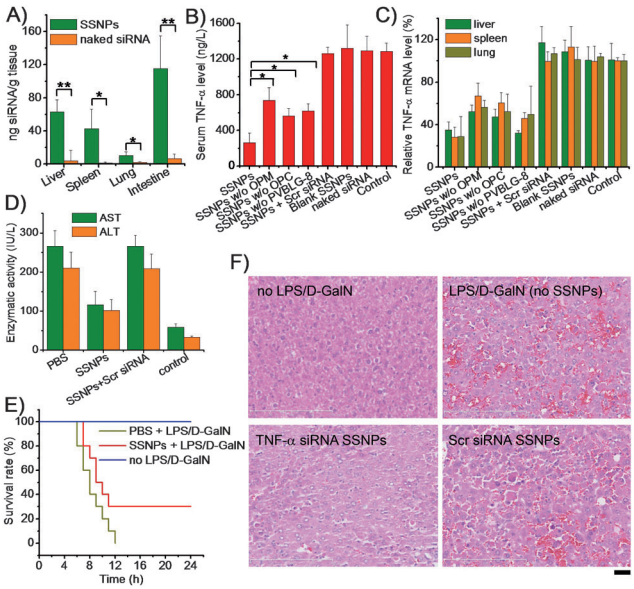

Figure 4. Orally delivered SSNPs mediated efficient RNAi against LPS-induced TNF-α production and protected mice from acute hepatic injury. A) Biodistribution of DY800-siRNA 2 h after oral gavage of SSNPs or naked DY800-siRNA ($n=3$). B) Serum TNF-α level of mice gavaged with SSNPs at 200 μg siRNA kg^{-1} ($n=6$). C) Relative TNF-α mRNA levels in mouse liver, spleen, and lung 24 h after oral gavage of SSNPs ($n=3$). D) Serum ALT and AST levels of mice 5 h after LPS/D-GalN stimulation ($n=4$). E) Survival of mice following oral gavage of SSNPs and i.p. injection of LPS/D-GalN 24 h later ($n=10$). (F) HE-stained liver sections from mice 5 h after LPS/D-GalN stimulation (bar = 1 mm).

livers remained normal reddish color, suggesting alleviation of the hepatic injury. Histological observation on HE-stained liver sections further confirmed the remarkable therapeutic efficacy of SSNPs in alleviating inflammatory symptoms, including congested central vein, infiltrated inflammatory cells, disarranged hepatocytes, and broken cytolemma (Figure 4F). It was also noted that 24 h following oral administration of SSNPs, serum IL-1β, IL-6, TNF-α, and IFN-γ levels were not significantly increased (Figure S19 in the Supporting Information), indicating that SSNPs and TNF-α siRNA did not activate pro-inflammatory cytokines or induce IFN-γ responses.

Single gavage of SSNPs to induce marked TNF-α silencing at a low dose of 200 μg siRNA kg^{-1} demonstrated comparable efficacy to that of previously reported β1,3-D-glucan particles (GeRPs), which required a cumulative dose of 160 μg siRNA kg^{-1} by oral administration within eight consecutive days.[19] For clinical application, oral administration is clearly superior to i.p. or i.v. injections for existing siRNA delivery systems in treating TNF-α-associated hepatic injury.[37,38] Although oral RNAi against TNF-α has been reported to treat bowel inflammation,[16,18,39] the gene knockdown was localized intestinally rather than infiltrated systemically, presumably due to inefficient intestinal absorption. Therefore, SSNPs that mediate effective intestinal absorption and systemic TNF-α silencing display obvious advantages. A relative pharmacological bioavailability of about 10% was noted compared to i.v. injection (comparable TNF-α silencing efficiency between oral gavage at 200 μg siRNA kg^{-1} and i.v.

administration at 20 μg siRNA kg^{-1}, Figure S17 in the Supporting Information), which suggested that oral administration represented a desired delivery route for systemic TNF-α silencing using multifunctional SSNPs. After SSNPs were intestinally absorbed by M cells, they could be directly transferred to the underlying GAMs which infiltrated systemic reticuloendothelial tissues to exert systemic gene knockdown.[19] With the OTMC/OPC-mediated mucoadhesion and OPM-mediated mannose-targeting, SSNPs could be efficiently taken up by M cells and thereafter be directed to the underlying GAMs. Their excellent gene silencing capability thus allowed potent TNF-α knockdown in GAMs and macrophages enriched in the liver, spleen, and lung, ultimately leading to systemic TNF-α depletion.

In summary, we have rationally designed and developed multifunctional SSNPs using a supramolecular self-assembly approach to incorporate materials with specific functions of mucoadhesion, transepithelial permeation, membrane penetration, and active targeting, which collectively contributed to the effective circumvention of the various gastrointestinal, systemic, and cellular barriers toward oral RNAi. To the best of our knowledge, no other nanoparticle-based delivery vehicle has been reported so far that possesses all of these attributes, making SSNPs the first example of a nanocarrier that simultaneously addresses the material requirements for mediating effective oral RNAi with a siRNA dose as low as 50 μg kg^{-1} (Figure S18 in the Supporting Information). The potent RNAi efficiency of SSNPs against systemic TNF-α production provides an exciting approach for the treatment of hepatic injury and other inflammatory diseases.

Received: December 14, 2012
Published online: April 22, 2013

Keywords: inflammation · nanoparticles · siRNA · supramolecular self-assembly · TNF-α

[1] C. Dulsat, N. Mealy, *Drugs Future* **2009**, *34*, 352.
[2] M. E. Davis, J. E. Zuckerman, C. H. J. Choi, D. Seligson, A. Tolcher, C. A. Alabi, Y. Yen, J. D. Heidel, A. Ribas, *Nature* **2010**, *464*, 1067.
[3] H. Lee, A. K. R. Lytton-Jean, Y. Chen, K. T. Love, A. I. Park, E. D. Karagiannis, A. Sehgal, W. Querbes, C. S. Zurenko, M. Jayaraman, C. G. Peng, K. Charisse, A. Borodovsky, M. Manoharan, J. S. Donahoe, J. Truelove, M. Nahrendorf, R. Langer, D. G. Anderson, *Nat. Nanotechnol.* **2012**, *7*, 389.
[4] K. A. Woodrow, Y. Cu, C. J. Booth, J. K. Saucier-Sawyer, M. J. Wood, W. M. Saltzman, *Nat. Mater.* **2009**, *8*, 526.
[5] J. H. Kim, Y.-W. Noh, M. B. Heo, M. Y. Cho, Y. T. Lim, *Angew. Chem.* **2012**, *124*, 9808; *Angew. Chem. Int. Ed.* **2012**, *51*, 9670.
[6] M. Jayaraman, S. M. Ansell, B. L. Mui, Y. K. Tam, J. Chen, X. Du, D. Butler, L. Eltepu, S. Matsuda, J. K. Narayanannair, K. G. Rajeev, I. M. Hafez, A. Akinc, M. A. Maier, M. A. Tracy, P. R. Cullis, T. D. Madden, M. Manoharan, M. J. Hope, *Angew. Chem.* **2012**, *124*, 8657; *Angew. Chem. Int. Ed.* **2012**, *51*, 8529.
[7] S. J. Lee, M. S. Huh, S. Y. Lee, S. Min, S. Lee, H. Koo, J. U. Chu, K. E. Lee, H. Jeon, Y. Choi, K. Choi, Y. Byun, S. Y. Jeong, K. Park, K. Kim, I. C. Kwon, *Angew. Chem.* **2012**, *124*, 7315; *Angew. Chem. Int. Ed.* **2012**, *51*, 7203.
[8] M. S. Shim, S. H. Bhang, K. Yoon, K. Choi, Y. Xia, *Angew. Chem.* **2012**, *124*, 12069; *Angew. Chem. Int. Ed.* **2012**, *51*, 11899.
[9] D. L. Lewis, J. E. Hagstrom, A. G. Loomis, J. A. Wolff, H. Herweijer, *Nat. Genet.* **2002**, *32*, 107.
[10] H. B. Xia, Q. W. Mao, H. L. Paulson, B. L. Davidson, *Nat. Biotechnol.* **2002**, *20*, 1006.
[11] J. P. Dassie, X. Y. Liu, G. S. Thomas, R. M. Whitaker, K. W. Thiel, K. R. Stockdale, D. K. Meyerholz, A. P. McCaffrey, J. O. McNamara, P. H. Giangrande, *Nat. Biotechnol.* **2009**, *27*, 839.
[12] J. B. Lee, J. Hong, D. K. Bonner, Z. Poon, P. T. Hammond, *Nat. Mater.* **2012**, *11*, 316.
[13] L. Alvarez-Erviti, Y. Q. Seow, H. F. Yin, C. Betts, S. Lakhal, M. J. A. Wood, *Nat. Biotechnol.* **2011**, *29*, 341.
[14] K. A. Howard, S. R. Paludan, M. A. Behlke, F. Besenbacher, B. Deleuran, J. Kjems, *Mol. Ther.* **2009**, *17*, 162.
[15] S. S. Kim, C. T. Ye, P. Kumar, I. Chiu, S. Subramanya, H. Q. Wu, P. Shankar, N. Manjunath, *Mol. Ther.* **2010**, *18*, 993.
[16] D. S. Wilson, G. Dalmasso, L. X. Wang, S. V. Sitaraman, D. Merlin, N. Murthy, *Nat. Mater.* **2010**, *9*, 923.
[17] S. Lee, S. C. Yang, C. Y. Kao, R. H. Pierce, N. Murthy, *Nucleic Acids Res.* **2009**, *37*, e145.
[18] C. Kriegel, M. Amiji, *J. Control. Release* **2011**, *150*, 77.
[19] M. Aouadi, G. J. Tesz, S. M. Nicoloro, M. X. Wang, M. Chouinard, E. Soto, G. R. Ostroff, M. P. Czech, *Nature* **2009**, *458*, 1180.
[20] K. Bowman, R. Sarkar, S. Raut, K. W. Leong, *J. Control. Release* **2008**, *132*, 252.
[21] L. M. Ensign, R. Cone, J. Hanes, *Adv. Drug Delivery Rev.* **2012**, *64*, 557.
[22] K. Roy, H. Q. Mao, S. K. Huang, K. W. Leong, *Nat. Med.* **1999**, *5*, 387.
[23] H. Wang, S. T. Wang, H. Su, K. J. Chen, A. L. Armijo, W. Y. Lin, Y. J. Wang, J. Sun, K. Kamei, J. Czernin, C. G. Radu, H. R. Tseng, *Angew. Chem.* **2009**, *121*, 4408; *Angew. Chem. Int. Ed.* **2009**, *48*, 4344.
[24] T. A. Sonia, C. P. Sharma, *Chitosan for Biomaterials I* **2011**, *243*, 23.
[25] N. P. Gabrielson, J. J. Cheng, *Biomaterials* **2010**, *31*, 9117.
[26] H. Lu, J. Wang, Y. Bai, J. W. Lang, S. Liu, Y. Lin, J. Cheng, *Nat. Commun.* **2011**, *2*, 206.
[27] N. P. Gabrielson, H. Lu, L. C. Yin, D. Li, F. Wang, J. J. Cheng, *Angew. Chem.* **2012**, *124*, 1169; *Angew. Chem. Int. Ed.* **2012**, *51*, 1143.
[28] V. Fievez, L. Plapied, A. des Rieux, V. Pourcelle, H. Freichels, V. Wascotte, M. L. Vanderhaeghen, C. Jerome, A. Vanderplasschen, J. Marchand-Brynaert, Y. J. Schneider, V. Preat, *Eur. J. Pharm. Biopharm.* **2009**, *73*, 16.
[29] L. C. Yin, J. Y. Ding, C. B. He, L. M. Cui, C. Tang, C. H. Yin, *Biomaterials* **2009**, *30*, 5691.
[30] M. Amarzguioui, P. Lundberg, E. Cantin, J. Hagstrom, M. A. Behlke, J. J. Rossi, *Nat. Protoc.* **2006**, *1*, 508.
[31] H. Katas, H. O. Alpar, *J. Control. Release* **2006**, *115*, 216.
[32] I. Kadiyala, Y. H. Loo, K. Roy, J. Rice, K. W. Leong, *Eur. J. Pharm. Sci.* **2010**, *39*, 103.
[33] Y. H. Loo, C. L. Grigsby, Y. J. Yamanaka, M. K. Chellappan, X. Jiang, H. Q. Mao, K. W. Leong, *J. Control. Release* **2012**, *160*, 48.
[34] Y. H. Lin, K. Sonaje, K. M. Lin, J. H. Juang, F. L. Mi, H. W. Yang, H. W. Sung, *J. Control. Release* **2008**, *132*, 141.
[35] I. A. Khalil, K. Kogure, H. Akita, H. Harashima, *Pharmacol. Rev.* **2006**, *58*, 32.
[36] L. Dong, S. H. Xia, Y. Luo, H. J. Diao, J. Zhang, J. N. Chen, J. F. Zhang, *J. Control. Release* **2009**, *134*, 214.
[37] P. Lundberg, H. J. Yang, S. J. Jung, M. A. Behlke, S. D. Rose, E. M. Cantin, *J. Control. Release* **2012**, *160*, 194.
[38] K. Un, S. Kawakami, M. Yoshida, Y. Higuchi, R. Suzuki, K. Maruyama, F. Yamashita, M. Hashida, *Hepatology* **2012**, *56*, 259.
[39] H. Laroui, A. L. Theiss, Y. T. Yan, G. Dalmasso, H. T. T. Nguyen, S. V. Sitaraman, D. Merlin, *Biomaterials* **2011**, *32*, 1218.

